SUPPORTING INFORMATION

Urban Aerosol Size Distributions over the Mediterranean City of Barcelona, Spain

M. Dall'Osto, D.C.S. Beddows, J. Pey, S. Rodriguez, A. Alastuey, R.M. Harrison and X. Querol

Aerosol size distribution clusters presented unique features within the same aerosol category; therefore each individual cluster is presented in this section, whereas a discussion on each category is instead presented in main manuscript (Results and Discussion).

- Cluster 1 (8%): it presents a bimodal size distribution with a major mode at 26±1nm and a smaller accumulation mode at 63±8nm. Cluster 1 presents intermediate values of gaseous pollutants, but has the feature of being associated with the lowest PM_1 (14±8 µg m^{-3}), $PM_{2.5}$ (18±10 µg m^{-3}) and PM_{10} (32±20 µg m^{-3}) concentrations. It is also associated with generally low temperature (16.1±6°), the lowest atmospheric pressure (1002±50mb) and the highest WS at ground level (2.7±1.8 m s^{-1}). Wind roses for this cluster points to a westerly direction and the diurnal profile is associated with traffic activity. This cluster did not present a clean annual seasonality, but it was found to be strongly associated with Atlantic air masses (64% of the time). We associate this cluster with local pollution diluted by clean Atlantic air.

- Cluster 2 (4%): it shows a similar aerosol size distribution to cluster 1, but the nanoparticle mode is about 25% smaller (20±13nm). Two additional modes can be seen, a broad Aitken mode at 30±25nm and an accumulation mode at 69±13nm. Whilst cluster 2 presented similar concentration of CO relative to cluster 1, lower values of NO (11±6 µg m^{-3}), NO_2 (25±20 µg m^{-3}), NO_x (41±30 µg m^{-3}) and SO_2 (1.6±1.5 µg m^{-3}) are notable. Compared to cluster 1, cluster 2 presented a lower NO_x/CO ratio ($11x10^{-3}$) and a higher NO_2/NO ratio (23). By contrast, higher ozone concentrations were seen for cluster 2 relative to cluster 1. Generally, similar values of PM loading were seen for cluster 1 and

cluster 2. Regarding meteorological parameters, higher temperature (21.2±7° - the third highest of all clusters), drier conditions (58±18%) and higher solar radiation values (284±300 W m^{-2}) were recorded for cluster 2 relative to cluster 1. Wind directions for this cluster were found mainly coming from the westerly sector. In contrast to cluster 1, cluster 2 showed a temporal profile starting to rise during traffic rush hours at 8am but continuing until about 1pm. Air masses associated with this cluster showed a more south westerly origin (Atlantic West and NAF, Table 4) relative to the more North Atlantic air masses associated with cluster 1. Finally, cluster 2 peaked during summer and autumn relative to the colder months of main occurrence of cluster 1. As with cluster 1, we associate cluster 2 with local pollution diluted by Atlantic air.

- Cluster 3 (16%): it shows a bimodal size distribution with a more dominant Aitken mode at 63±3nm and a smaller nanoparticle mode at 22±1nm. This cluster did not present a close correlation with any gaseous pollutant, nor with particulate mass or meteorological data. It was associated with south-south westerly winds. It was detected mainly during summer and autumn months and was not found to be associated with any specific air mass back trajectory. This cluster was the least well characterised of all the nine.

- Cluster 4 (26%): The major mode is in the nanoparticle range, dominating both N and V concentrations. This cluster is associated with the most polluted conditions, with highest concentrations of CO (0.6±0.5 mg m^{-3}) and NO_2 (42±25 µg m^{-3}), but the lowest ozone concentrations (29±24 µg m^{-3}). Concentrations of PM_1 and $PM_{2.5}$ were generally high with the second highest mean PM_{10} concentration (40±27 µg m^{-3}) associated. This cluster presented the lowest temperature (15.9±5°) and the lowest solar radiation values

(136±222W m^{-2}). Easterly wind directions and diurnal temporal profiles associated with traffic, along with higher occurrence during winter months and Atlantic air masses (66%) were further characteristics of this cluster. We attribute this cluster to winter traffic emissions.

- Cluster 5 (27%): this cluster is the most frequent of all, with a bimodal size distribution peaking at 29±1 and 78±5 nm, respectively. It is associated with high gaseous pollutant concentrations, the second highest of all clusters after cluster 4. Similar trends can be seen for the PM loadings. Relative to cluster 4, cluster 5 was associated with slightly higher temperatures (16.9±6°), RH (70±15%), solar radiation (145±200 W m^{-2}) and atmospheric pressure (1006.4±38 mb). Winds were found to be mainly from the west and north east. Diurnal profiles were similar to cluster 4, and slightly less pronounced during traffic rush hours. It did not present a clear seasonality nor a clear air mass back trajectory trend. Like cluster 4, we associate cluster 5 with traffic emissions.

- Cluster 6 (2%): This cluster presented unique properties. It was associated with the lowest gaseous primary pollutant concentrations (0.3±0.1 for CO, 6±5 for NO, 18.9±10 for NO_x, 1.5±1.6 for SO_2; CO in mg m^{-3}, all others in µg m^{-3}) and the highest ozone concentrations (73±21 µg m^{-3}). Masses of PM_1 and $PM_{2.5}$ (18±7, 22±7 µg m^{-3}, respectively) were the third lowest of all clusters whilst coarse PM_{1-10} was the lowest of the nine clusters (17±7 µg m^{-3}). Cluster 6 presented the highest average temperature (27.2±4°) and the strongest solar radiation (487±300 W m^{-2}), and the second strongest WS at the Fabra Observatory (5.9±2.2 m s^{-1}). Wind roses were found strongly pointing south west, typical of sea breeze conditions. The diurnal temporal variation was found to

spike between 1pm and 4pm, with major occurrence during the months of July and August (68%). Additional unique features of this cluster were the highest occurrence during daylight of all the clusters (95%), the highest ratio weekend over weekdays of all clusters, the highest NO_2/NO ratio (2.5±0.3) and the lowest NO_x/CO ratio (50±10x10^{-3}). Finally, 48% of the time this cluster was detected it was associated with regional summer air masses. We attribute this cluster to photochemical nucleation events occurring during summertime.

- Cluster 7 (10%): it shows a bimodal size distribution for this cluster with two modes at 32±1 and 90±3nm, respectively. Generally, it presented the fourth highest concentrations for CO (0.5±0.3 mg m^{-3}), NO (32±35 mg m^{-3}), NO_x (83±10 µg m^{-3}) and NO_2 (34±26 µg m^{-3}) but the second strongest SO_2 concentration (4.7±7 µg m^{-3}). It presented the highest PM loadings of all twelve clusters: PM_1 of 32±18 µg m^{-3}, $PM_{2.5}$ of 38±21 µg m^{-3} and PM_{10} of 52±30 µg m^{-3}. The generally low temperature (17±7°) was coupled with the highest RH and the highest atmospheric pressure of all clusters (70±15% and 1010±50mb, respectively). Whilst the wind rose was not well defined for this cluster, the diurnal profile was heavily biased towards nighttime hours. Fig. SI2 shows a seasonality peaking during colder months, with the highest regional winter episode air masses associated with this cluster. Finally, this cluster was found to present the lowest day time occurrence (40%) among all clusters as well as the highest PM_1/PM_{10} ratio (0.62). We attributed this cluster to regional winter pollution events.

- Cluster 8 (2%): it shows the lowest particle number concentrations associated with this cluster, with a tri-modal distribution at 20±1, 80±1 and 237±22nm. However, the major mode is represented by the middle Aitken one. This cluster presents similar properties to cluster 6: very low concentrations of primary gaseous pollutants (0.3±0.1 for CO, 10±20

for NO, 12±10 for NO_2 and1.4±1.2 for SO_2; CO in mg m^{-3}, all others in µg m^{-3}) and the second highest ozone concentration (66±21 µg m^{-3}). Generally low values of PM loadings are associated with this cluster. The meteorological parameters associated with this cluster also reflect the ones encountered for cluster 6, with the second highest average temperature (24.1±6°), the second highest average solar radiation (322±300 W m^{-2}) and the strongest WS (6.3±3 m s^{-1}). It was associated with wind roses identical to cluster 6 (south west) and again a strong seasonality with highest occurrence during the months of July and August. It was associated with regional summer air masses (35%) and was detected 75% of the time during daylight reflecting again features of cluster 6. However, the diurnal profile of this cluster 8 spikes later than cluster 6, at around 3-6pm. As with cluster 6, we attribute this cluster to photochemical nucleation events although this cluster likely is associated with growth events as discussed in the next section.

- Cluster 9 (5%): This cluster was the only one of all twelve presenting a unimodal aerosol size distribution peaking at 55±1nm. This cluster had the highest gas phase pollutant concentrations for CO (0.6±0.6 mg m^{-3}), NO (47±70 µg m^{-3}), NO_x (111±40 µg m^{-3}) and SO_2 (5.6±5 µg m^{-3}). It was associated with the second highest concentrations of PM_1 (22±6 µg m^{-3}) $PM_{2.5}$ (28±14 µg m^{-3}) and PM_{10} (44±17 µg m^{-3}), respectively. Meteorological data did not show any specific trends whereas wind roses pointed to the south east. The diurnal profile for this cluster is shifted towards daylight hours. Interestingly, cluster 9 presented a clear seasonality profile peaking during summer months. Among with cluster 7, it presented the highest NO_x/CO ratio (about $140x10^{-3}$). We attribute this cluster to summer regional pollution events.

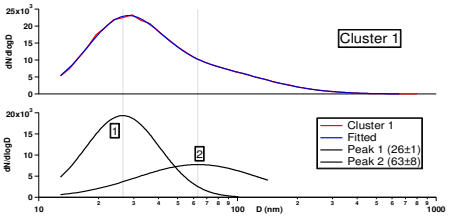
Cluster 1
dN/dlogD
Cluster 1
Fitted
Peak 1 (26±1)
Peak 2 (63±8)
D (nm)

(a)

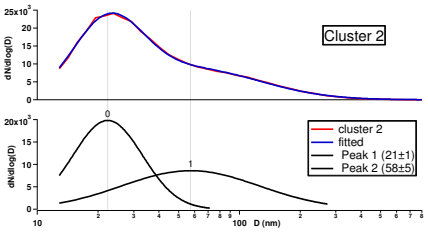
Cluster 2
dN/dlog(D)
cluster 2
fitted
Peak 1 (21±1)
Peak 2 (58±5)
D (nm)

(b)

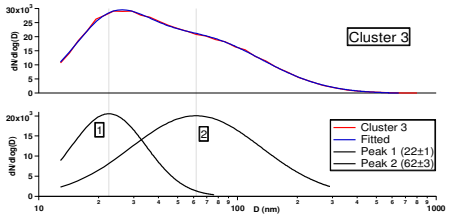
Cluster 3
dN/dlog(D)
Cluster 3
Fitted
Peak 1 (22±1)
Peak 2 (62±3)
D (nm)

(c)

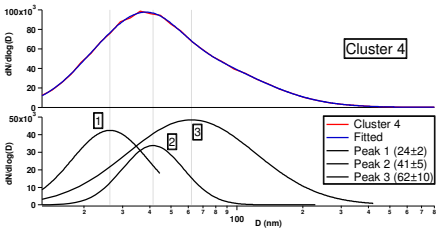
Cluster 4
dN/dlog(D)
Cluster 4
Fitted
Peak 1 (24±2)
Peak 2 (41±5)
Peak 3 (62±10)
D (nm)

(d)

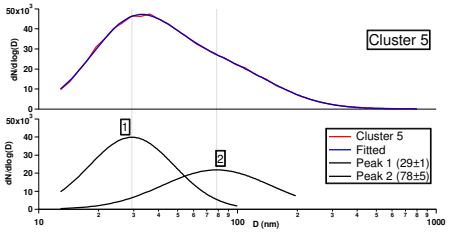
Cluster 5
dN/dlog(D)
Cluster 5
Fitted
Peak 1 (29±1)
Peak 2 (78±5)
D (nm)

(e)

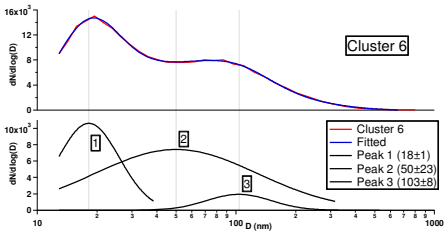
Cluster 6
dN/dlog(D)
Cluster 6
Fitted
Peak 1 (18±1)
Peak 2 (50±23)
Peak 3 (103±8)
D (nm)

(f)

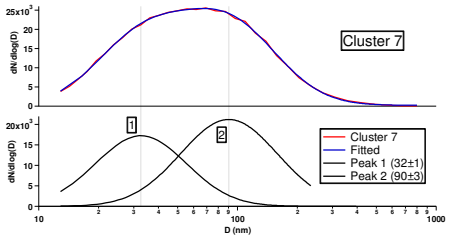
Cluster 7
dN/dlog(D)
Cluster 7
Fitted
Peak 1 (32±1)
Peak 2 (90±3)
D (nm)

(g)

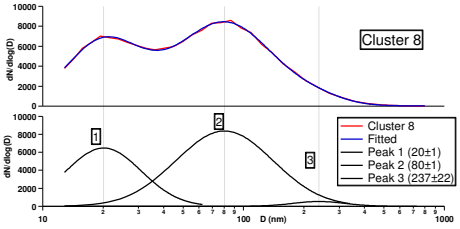
Cluster 8
dN/dlog(D)
Cluster 8
Fitted
Peak 1 (20±1)
Peak 2 (80±1)
Peak 3 (237±22)
D (nm)

(h)

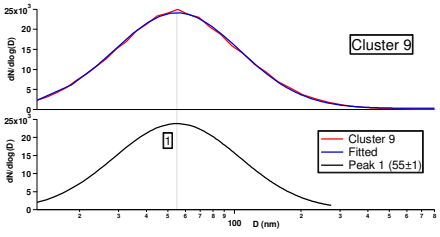
Cluster 9
dN/dlog(D)
Cluster 9
Fitted
Peak 1 (55±1)
D (nm)

(i)

Figure SI1(a-i). Disaggregation of the aerosol size distributions of the nine SMPS clusters (dN/dlog(D) - cm^{-3}). Top shows the real (red) and the fitted (blue) total aerosol size distributions, bottom the log-normal peak fittings. Brackets of each peak fitting represents log normal peak location and precision (nm)

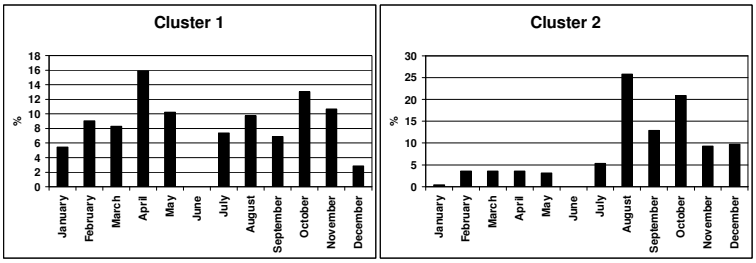

(a)

(b)

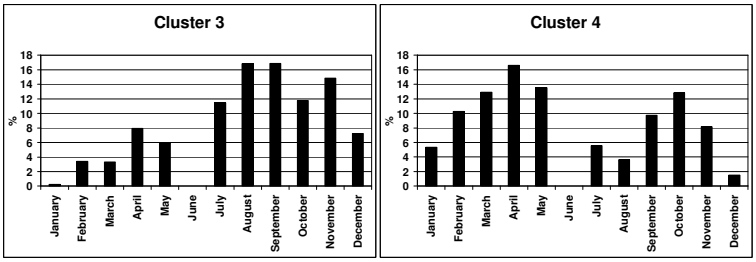

(c)

(d)

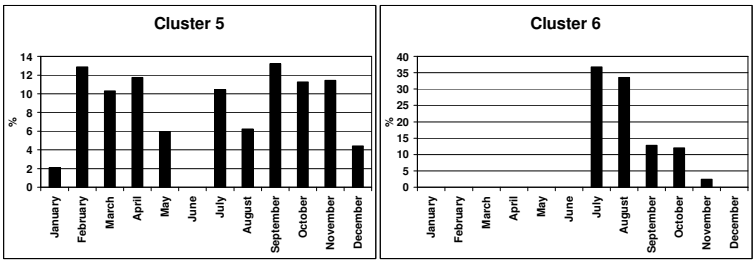

(e)

(f)

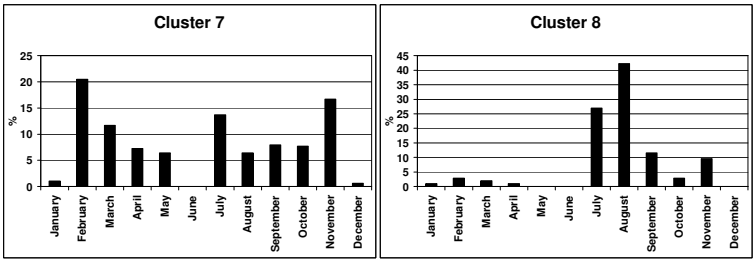

(g)

(h)

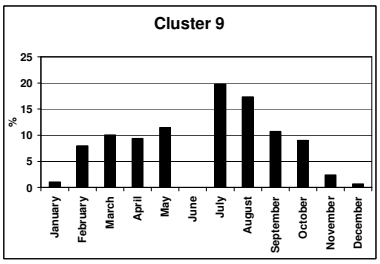

(i)

Figure SI2. Occurrence of each of the 9 clusters (a-i) for each month of the year. Please note June did not have measurements and January and December very few (Table 1)